*SF2A 2007*
*J. Bouvier, A. Chalabaev, C. Charbonnel (eds)*

# ON TYPE I PLANETARY MIGRATION IN AN ADIABATIC DISK

C. Baruteau[1] and F. Masset[1]

**Abstract.** A low mass planet embedded in a circumplanetary disk should undergo a fast orbital decay towards the central object. This process, known as type I migration, has been extensively studied analytically and numerically, assuming that the disk is either barotropic, or described with a locally isothermal equation of state. We investigate in this communication the case of an adiabatic disk, by means of two-dimensional hydrodynamic simulations. Entropy perturbations, that are advected in the planet's coorbital region, yield an excess of corotation torque that scales with the initial entropy gradient at corotation. This excess can be large enough to slow down the migration process significantly, or even stop it.

## 1 Context and numerical setup

Recently, Paardekooper & Mellema (2006) have revisited the type I migration with high resolution three-dimensional calculations, including radiative transfer. They find that the total torque exerted by the disk on the planet increases with the disk opacity. For sufficiently large values of the opacity (and in the limit case of an adiabatic flow, corresponding to an infinite opacity), they find that the total torque on the planet is positive. This result is of great importance, as it potentially solves the lingering problem of type I migration. The present work corresponds to an attempt to further investigate this topic, so as to identify the physical mechanism responsible for these effects. For this purpose, we consider a more restricted situation, namely two-dimensional adiabatic flows.

Our numerical simulations are performed with the code FARGO (Masset 2000). It is a staggered mesh hydrocode that solves the Navier-Stokes and continuity equations on a polar grid. A locally isothermal equation of state is used to close the hydrodynamic equations: the vertically integrated pressure $p$ of the disk and its surface density $\Sigma$ are connected with $p = \Sigma c_{s,\mathrm{iso}}^2$, where $c_{s,\mathrm{iso}}$ denotes the isothermal sound speed.

In this communication, we investigate the case of an inviscid, radiatively inefficient disk, in the adiabatic limit. For this purpose, we implemented in FARGO an energy equation that is equivalent to the Lagrangian conservation of the gas entropy $S$, defined as $S = p\Sigma^{-\gamma}$. The hydrodynamic equations are closed by the equation of state $p = \Sigma c_{s,\mathrm{adi}}^2/\gamma$, where the adiabatic index $\gamma$ is set to 1.4 and $c_{s,\mathrm{adi}} = \sqrt{\gamma}\, c_{s,\mathrm{iso}}$ denotes the adiabatic sound speed.

In this work, we aim at comparing the disk's response to the introduction of a low mass planet, the disk being described either by a locally isothermal equation of state, or by an adiabatic energy equation. The isothermal and adiabatic calculations have same initial surface density and temperature profiles. Figure 1 yields an overview of the disk's response in both situations. It represents the relative perturbation of the disk surface density with respect to the initial, unperturbed state. Two main differences can be highlighted:

1. The wake generated by the planet is less tightly wound when an adiabatic energy equation is taken into account, since the adiabatic sound speed is greater than the isothermal one. We comment that the differential Lindblad torque, which scales as $c_s^{-2}$ (Ward 1997), is therefore weakened by a factor of $\gamma$ in an adiabatic disk. The same is true of the corotation torque, when there is no entropy gradient.

2. The adiabatic situation displays an additional density structure, located in a narrow annulus surrouding the planet. This structure can have a dramatic impact on the corotation torque, as we shall see.

[1] Laboratoire AIM, CEA/DSM - CNRS - Université Paris Diderot, DAPNIA/Service d'Astrophysique, CEA/Saclay, 91191 Gif/Yvette Cedex, France

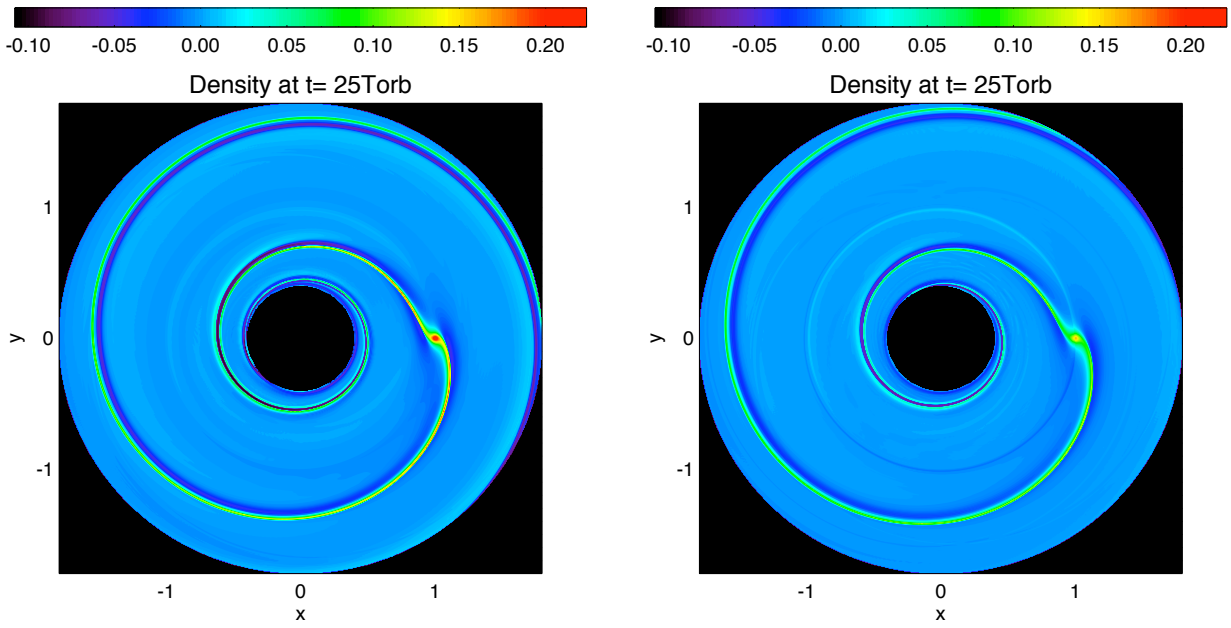


**Fig. 1.** Relative perturbation of the gas surface density, after 25 planet orbital periods, obtained with the isothermal calculation (left panel) and the adiabatic calculation (right panel). In this cartesian representation, the planet is located in $x = 1$, $y = 0$. The color scale is identical in both panels so as to highlight their differences (see text).

## 2 Excess of corotation torque and entropy gradient

We first present the results of an illustrative calculation with a $q = 2.2 \times 10^{-5}$ planet to primary mass ratio (corresponding to a $M_p = 7.3\ M_\oplus$ planet mass if the central object has a solar mass). The planet is held on a fixed circular orbit, at $r = r_p$, and our reference frame corotates with the planet. Two calculations were performed: an adiabatic and an isothermal one. For both calculations, the unperturbed pressure $p_0$ and surface density $\Sigma_0$ are power laws of the radius, respectively with index $\lambda$ and $\sigma$: $p_0(r) \propto r^{-\lambda}$ and $\Sigma_0(r) \propto r^{-\sigma}$. The initial entropy $S_0$ therefore scales as $r^{\gamma\mathcal{S}}$, with $\mathcal{S} = \sigma - \lambda/\gamma$. For this example, we took $\sigma = 0.5$ and $\lambda = 1.1$, so that $\mathcal{S} \sim -0.3$.

Figure 2 displays the gas entropy, pressure and surface density obtained with the adiabatic calculation, after 25 planet orbital periods. Each panel represents the relative perturbation of the corresponding quantity with respect to the unperturbed state. For instance, the left panel shows $[S(r,\varphi) - S_0(r)]/S_0(r)$, with $r$ and $\varphi$ the polar coordinates. While the azimuthal range spans the whole $[0, 2\pi]$ interval, the radial range depicted is restricted to a band of width $2.5x_s$ around the corotation radius, where $x_s$ denotes the half-width of the planet's horseshoe region. Streamlines are overplotted to the entropy panel to give an idea of the extent of the horseshoe region. The vertical dashed line represents the corotation radius $r_c$. Whereas the pressure panel does not display any significant perturbation, the entropy and density panels show the propagation of a perturbation inside the horseshoe region, which slides along the separatrices.

The interpretation of this dynamics is as follows: the entropy of the fluid elements is conserved as they perform a horseshoe U-turn in the co-orbital region. When there is initially an entropy gradient at corotation, the co-orbital dynamics yields an entropy perturbation that has a sign opposite of that of the entropy gradient on the outwards U-turns, and the sign of the entropy gradient on the inwards U-turns. In the example shown here, there is initially a negative entropy gradient at corotation: the co-orbital dynamics yields a positive entropy perturbation at $\varphi < \varphi_p$ and a negative entropy perturbation at $\varphi > \varphi_p$. Since the pressure field is only weakly perturbed, the entropy perturbation is related to a density perturbation of opposite sign and, in relative value, of same order of magnitude. Baruteau & Masset (2007) showed that these perturbations arise only in adiabatic disks, where a non-vanishing entropy gradient induces a singularity in the entropy and surface density fields at corotation, while the pressure field is continuous. This contact discontinuity, as we shall call it, is simply advected by the flow: here, it follows the horseshoe dynamics and it remains confined to the horseshoe region.

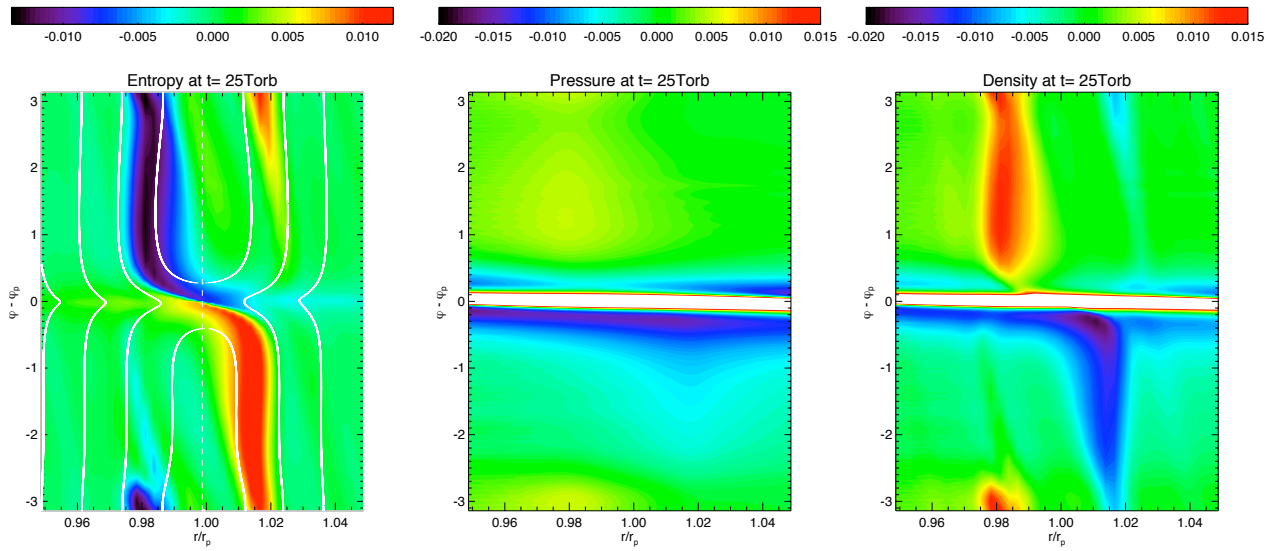


**Fig. 2.** Relative perturbations of the gas entropy, pressure and surface density, at $t = 25$ orbital periods, obtained with the adiabatic calculation. In this polar framework, the planet is located in $r = r_p$, $\varphi = \varphi_p$. In the left panel, streamlines are overplotted and the vertical dashed line stands for the corotation radius. In the middle and right panels, the color scale is adjusted to highlight the advection of entropy perturbation in the horseshoe region (see text). The nearly horizontal overdensity structure at $\varphi = \varphi_p$ is the protoplanet's wake.

Such perturbations do not exist in the isothermal situation since neither the entropy is conserved along a fluid element path, nor is a temperature singularity allowed to appear.

We give hereafter a simple estimate of the relative perturbation of the disk surface density due to the advection of entropy. We consider a fluid element that performs a horseshoe U-turn from the inner part of the horseshoe region (where we assume that there is no entropy perturbation, which is true as long as $t < \tau_{\rm lib}/2$, $\tau_{\rm lib}$ denoting the horseshoe libration time) to the outer part. All physical quantities at the inner (outer) leg of the horseshoe streamline are denoted by a minus (plus) subscript. Assuming no pressure perturbation, a first-order expansion yields $p_\pm = p_0(r_c)(1 \mp \lambda x/r_c)$, where $0 < x < x_s$ is the distance of the streamline to corotation, and $\Sigma_- = \Sigma_0(r_c)(1 + \sigma x/r_c)$. On the outer horseshoe leg, the disk surface density is perturbed according to the entropy perturbation and reads $\Sigma_+ = \Sigma_0(r_c)(1 + R - \sigma x/r_c)$, where $R$ is the relative perturbation of surface density at $r = r_c + x$ (we assume a symmetric horseshoe U-turn), due to the entropy advection. Entropy conservation along the fluid element path ($S_- = S_+$) leads to:

$$R = 2\frac{x}{r_c}\left(\sigma - \frac{\lambda}{\gamma}\right) = 2\frac{x}{r_c}\mathcal{S}. \tag{2.1}$$

The horseshoe U-turn that we have considered lags the planet ($\varphi < \varphi_p$). A similar conclusion holds for a horseshoe U-turn that switches from the outer leg to the inner one (at $\varphi > \varphi_p$), hence we finally have:

$$R(x) = 2x\mathcal{S}/r_c,\ \forall x \in [-x_s, +x_s]. \tag{2.2}$$

We display in Fig. 3 the slices of the perturbed density field of Fig. 2c, for $\varphi - \varphi_p = 1$ (diamonds) and $\varphi - \varphi_p = -1$ (stars). The two horizontal dashed lines display the values of $R(-x_s)$ and $R(x_s)$, where $x_s$ is estimated through a streamline analysis. Similarly, the long-dashed curve shows $R(x) = 2x\mathcal{S}/r_c$, which is in correct agreement with the calculation results. The surface density structure in the horseshoe region is therefore dictated by the sign of $\mathcal{S}$. In particular, we do not expect any contact discontinuity when $\mathcal{S} = 0$, which we checked with appropriate calculations.

We now examine the impact of the contact discontinuity on the corotation torque. The left panel of Fig. 4 shows the total torque exerted on the planet, as a function of time, obtained with the adiabatic and isothermal calculations. The dashed curve depicts the isothermal torque rescaled by a factor $\gamma^{-1}$. It corresponds to the

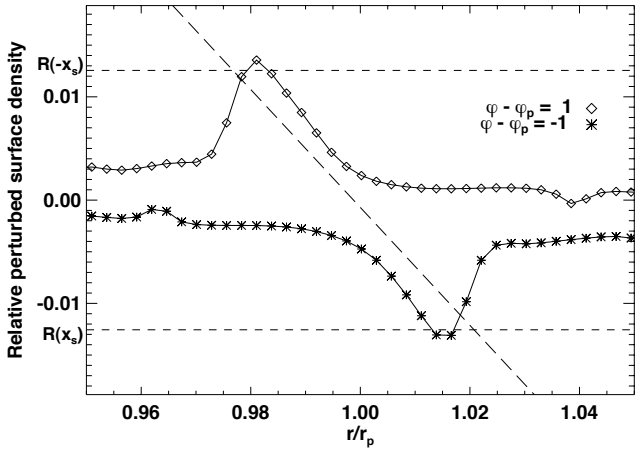


**Fig. 3.** Slices of the relative perturbed density field depicted in Fig. 2c, at $\varphi - \varphi_p = 1$ (diamonds) and $\varphi - \varphi_p = -1$ (stars). The two horizontal dashed lines refer to the values of $R(-x_s)$ and $R(x_s)$, while the long-dashed curve displays the quantity $2(r - r_c)\mathcal{S}/r_c$ (see text and Eq. (2.2)).

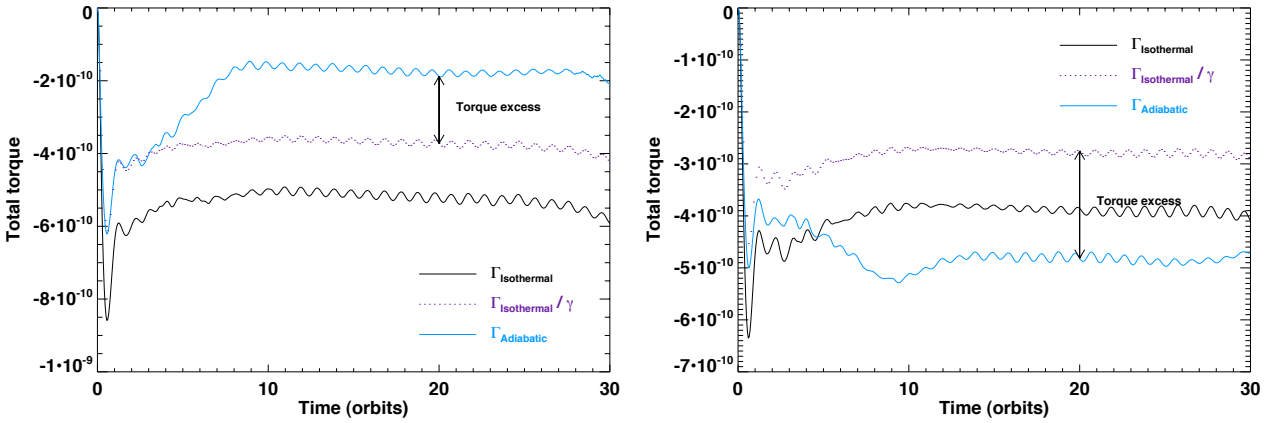


**Fig. 4.** Total torque exerted on the planet, obtained with the adiabatic and isothermal calculations, for $\mathcal{S} \sim -0.3$ (left panel) and $\mathcal{S} \sim 0.3$ (right panel). The dashed curve represents the isothermal torque divided by $\gamma$, and the vertical arrow displays the torque excess (see text).

torque expected in the adiabatic situation when discarding the surface density perturbation due to the contact discontinuity (see section 1). The adiabatic calculation displays a significant, positive torque excess after a few orbits. This torque excess accounts for the excess of corotation torque due to the contact discontinuity. It contributes in this exemple to reduce the total torque by as much as a factor of two.

Furthermore, the right panel of Fig. 4 displays the results of two additional isothermal and adiabatic calculations performed with $\mathcal{S} \sim 0.3$. As expected, the torque excess is this time negative, and its absolute value is very close to the one obtained with $\mathcal{S} \sim -0.3$. This suggests that the torque excess scales with $\mathcal{S}$, hence with the initial entropy gradient at corotation. To check this expectation, we have undertaken a number of calculations with different values of $\mathcal{S}$, with the same planet to primary mass ratio. Each entropy gradient is realized with different combinations of the indexes of the pressure and density power laws ($\lambda$ and $\sigma$). We calculate the torque excess by substracting the total torque of an adiabatic and an isothermal calculation, the isothermal torque being rescaled by $\gamma^{-1}$. The left panel of Fig. 5 confirms that the torque excess essentially scales with the initial entropy gradient.

The results of our calculations show that a negative entropy gradient yields a positive excess of corotation

torque in an adiabatic disk, which slows down type I migration. If the entropy gradient is sufficiently negative, the torque excess can be positive enough to yield a positive total torque, thereby reversing the migration process.

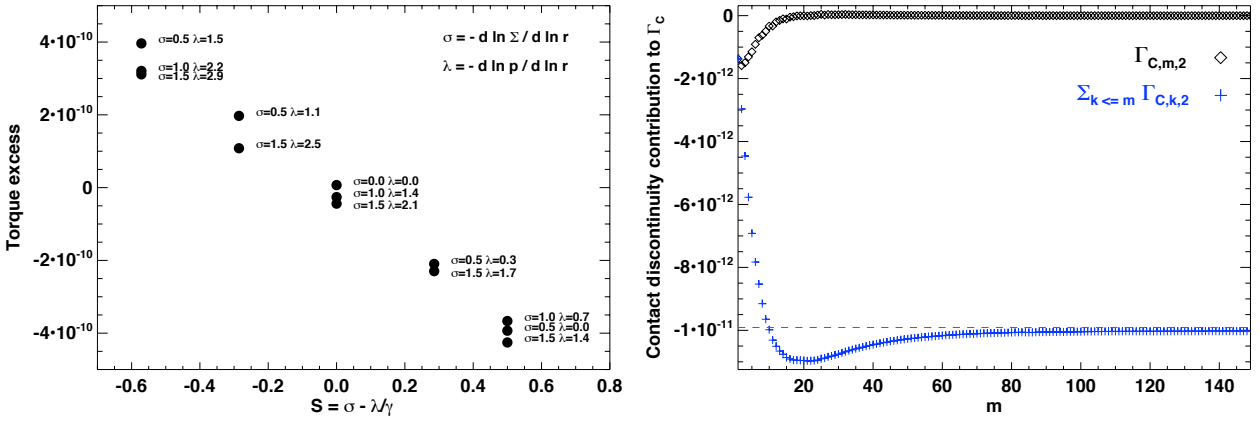


**Fig. 5.** Left: Torque excess as a function of $\mathcal{S}$. Although the calculations display some scatter for a given value of $\mathcal{S}$, the different points can be considered as aligned within a good level of accuracy. The slope of the dependence is negative. Right: Contact discontinuity contribution to the corotation torque. It is evaluated numerically with Eq. (3.4). The cumulative series (plus signs) tends to a value that is in excellent agreement with the contact discontinuity contribution obtained with numerical simulations, calculated as $\int_{\rm disk}(\Sigma_1 - p_1/c_s^2)\,\partial_\varphi\Phi\, r dr d\varphi$ (long-dashed curve).

## 3 Connection to analytics

We now aim at comparing the results of our calculations with analytical predictions. Namely, we study the linear response of an adiabatic disk to a rotating perturbing potential $\Phi(r,\varphi)$. Combining the Euler, continuity and energy (entropy) equations leads to a second-order differential equation for the perturbed[1] quantity $\Psi = p_1/\Sigma_0$, as a function of $\Phi$ and its radial derivatives. We calculate the rate of angular momentum exchanged by the disk and the perturber at the corotation radius $r_c$. This rate defines the corotation torque[2] $\Gamma_{\rm C}$. In the vicinity of corotation and assuming that $\Phi$ is real, the corotation torque takes the form[3] $\Gamma_{\rm C} = \sum_m \Gamma_{\rm C,m}$ with:

$$\Gamma_{\rm C,m} = m\pi r_c^2 \Phi(r_c) \int_{-\infty}^{\infty} dx\, {\rm Im}[\Sigma_1(x)], \tag{3.1}$$

where $x = (r - r_c)/r_c$. As in Goldreich & Tremaine (1979), we assume that the disk responds to a slowly increasing perturbation. Linearizing the energy equation leads to:

$$\Sigma_1(x) = \frac{p_1(x)}{c_{s,{\rm adi}}^2(r_c)} - (x + i\epsilon)^{-1} \left[\frac{2\mathcal{F}\mathcal{S}(\Phi+\Psi)}{r^3 d\Omega/dr}\right]_{r_c}, \tag{3.2}$$

where $\epsilon$ is an arbitrarily small positive quantity, $\mathcal{F} \approx \Sigma_0\Omega/\kappa^2$, $\Omega$ denotes the disk's rotation profile, $\kappa$ the epicyclic frequency. Each term of the r.h.s. of Eq. (3.2) yields a contribution to the corotation torque:

- the contribution of $p_1/c_s^2$, denoted $\Gamma_{\rm C,m,1}$. This contribution is calculated as the jump at corotation of the advected angular momentum flux (Tanaka et al. 2002). Its expression, that features $\Psi(r_c)$, reads:

$$\Gamma_{\rm C,m,1} = \left[\Gamma_0\left\{\mathcal{V} + 2\mathcal{S}\right\}|\Phi+\Psi|^2 - \Gamma_0\,\mathcal{S}\Phi{\rm Re}(\Phi+\Psi)\right]_{r_c}, \tag{3.3}$$

  where $\Gamma_0 = -(m\pi^2\Sigma_0)/(2Brd\Omega/dr) > 0$, $B = \kappa^2/4\Omega$ and $\mathcal{V} \equiv d\ln(\Sigma_0/B)/d\ln r$.

[1] Unperturbed (perturbed) quantities are referred to with a zero (one) subscript.
[2] Hereafter the torque means the torque exerted by the disk on the perturber.
[3] The subscript $m$ in the perturbed quantities is skipped to improve legibility.

- the contribution of the second term, denoted $\Gamma_{\rm C,m,2}$. In the limit $\epsilon \rightarrow 0$, this term corresponds to a singularity at corotation (the so-called contact discontinuity of previous section). It reads:

$$\Gamma_{\rm C,m,2} = -\left[\Gamma_0\, \mathcal{S}\, \Phi\, {\rm Re}(\Phi+\Psi)\right]_{r_c}. \tag{3.4}$$

The corotation torque therefore reads:

$$\Gamma_{\rm C,m} = \left[\Gamma_0\ \{\mathcal{V}+2\mathcal{S}\}\,|\Phi+\Psi|^2 - 2\Gamma_0\,\mathcal{S}\Phi{\rm Re}(\Phi+\Psi)\right]_{r_c}. \tag{3.5}$$

This expression reduces to the formula of Tanaka et al. (2002) when $\mathcal{S}=0$, and to that of Goldreich & Tremaine (1979) in the limit of a cold disk ($\Psi(r_c) \ll \Phi(r_c)$).

This linear analysis leads to the following comments:

1. The torque excess, which we denote by $E$, reads: $E = \Gamma_{\rm C,m} - [\Gamma_0\,\mathcal{V}\,|\Phi+\Psi|^2]_{r_c}$. Assuming that $0 \leq \Psi(r_c) \approx -\Phi(r_c)$, $E$ can be recast as: $E \approx -2[\mathcal{S}\Gamma_0\Phi{\rm Re}(\Phi+\Psi)]_{r_c}$. The torque excess does scale with $-\mathcal{S}(r_c)$, as inferred from our results of calculations (see left panel of Fig. 5).

2. We have given at Eq. (3.4) an estimate of the singular torque contribution from the contact discontinuity at an isolated resonance. We now compare the sum over $m$ of this torque expression with the total contribution in the planetary case of the contact discontinuity, evaluated as: $\Gamma_{\rm cd} = \int_{\rm disk}(\Sigma_1 - p_1/c_s^2)\,\partial_\varphi\Phi\, r dr d\varphi$. For this purpose, we have adopted a planet to primary mass ratio $q = 5\times10^{-6}$, as the one adopted in the previous section ($q = 2.2\times10^{-5}$) led to poor agreement, presumably because of the onset of non-linear effects. For each azimuthal wavenumber $m$, we measure $\Re(\Psi_m)$ from the calculation output (at $t = 5\,T_{\rm orb}$), and we evaluate the sum over $m$ of the torque $\Gamma_{c,m,2}$: $\Gamma_\infty = \lim_{k\rightarrow+\infty}\Gamma'_k$, where:

$$\Gamma'_k = -\frac{4\pi^2}{3}\left[\frac{\mathcal{S}\Sigma_0}{\Omega^2}\right]_{r_c}\sum_{m=1}^{m\leq k} m\Phi_m[\Phi_m + \Re(\Psi_m)] \tag{3.6}$$

is the partial sum of $\Gamma_{c,m,2}$. We compare $\Gamma_{\rm cd}$ to $\Gamma_\infty$ in the right panel of Fig. 5. The agreement between the result of our calculation and the linear estimate is excellent, which confirms that the contact discontinuity is essentially a linear effect.

## 4 Conclusion

We investigate in this communication the type I planetary migration in an adiabatic disk. When the initial entropy gradient at corotation cancels out, the torque of an adiabatic calculation is reduced by a factor of $\gamma$ with respect to an isothermal calculation. When a non-vanishing entropy gradient is taken into account, a singularity appears in the entropy and surface density fields at corotation, which yields an additional contribution to the corotation torque. The close agreement between the results of our calculations and linear analysis shows that this effect is essentially a linear one. The excess of corotation torque scales with the initial entropy gradient at corotation: if the latter is sufficiently negative, the torque excess can be positive enough to reverse the migration.

## References

Baruteau, C., & Masset, F. 2007, ApJ, subm.

Goldreich, P., & Tremaine, S. 1979, ApJ, 233, 857

Masset, F. 2000, A&A, 141, 165

Paardekooper, S.-J., & Mellema, G. 2006, A&A, 459, L17

Tanaka, H., Takeuchi, T., & Ward, W. R. 2002, ApJ, 565, 1267

Ward, W. R. 1997, Icarus, 126, 261